Journal of Theoretical and Applied Information Technology

31st October 2023. Vol.101. No 20

ISSN: 1992-8645 www.jatit.org E-ISSN: 1817-3195

KIDNEY STONES IDENTIFICATION UTILIZING EXTREME LEARNING MACHINE

SHARFINA FAZA[1], ROMI FADILLAH RAHMAT[2*], MERYATUL HUSNA[1], AJULIO PADLY SEMBIRING[1], LISA FELICIA SILAEN[2], FARHAD NADI[3]

[1] Department of Computer Engineering and Informatics, Politeknik Negeri Medan, Indonesia

[2] Department of Information Technology, Universitas Sumatera Utara, Indonesia

[3] School of Information Technology, UNITAR International University, Malaysia

*Corresponding E-mail: romi.fadillah@usu.ac.id

ABSTRACT

The kidneys are two reddish-brown bean-shaped organs in humans. One of the diseases that attack the kidneys is kidney stones. Kidney stones occur when there are minerals or other substances in the blood that crystallize in the kidneys and form a solid. In identifying kidney stones, doctors and radiologists look at ultrasound images of the kidneys manually. Of course, doctors are experts at detecting them, but there is still the possibility of an error in predicting the images. For this reason, a computational method is needed to facilitate the identification of kidney stones suffered by patients through ultrasound images of the kidneys. This study aimed to identify kidney stones through ultrasound images using the Extreme Learning Machine method. The steps in conducting this research are Preprocessing, Segmentation, Feature Extraction, and Identification. In preprocessing Scaling and contrast enhancement is using CLAHE, in Segmentation uses Thresholding OTSU and Morphological Close segmentation methods, in feature extraction the method used is Gray Level Co-occurrence Matrix (GLCM) and identification with Extreme Machine Learning. This study obtained an accuracy of 92.30%. The contribution of this research is to show the ability of ELM in classifying kidney stone images, which will give initial identification before definite verdict from health specialist.

Keywords: *Kidney, Kidney Stones, Images, Gray Level Co-occurrence Matrix, Extreme Machine Learning*

1. INTRODUCTION

The kidneys are one of the excretory organs in humans. The kidneys' primary function for humans is to filter blood in the human body and remove excess fluid residues in the body [1]. One of the diseases that attack the kidneys is kidney stones. In 2013, 6 per 1000 population suffered from kidney stones, namely 1,499,400 Indonesians [2]. Kidney stones occur when minerals or other substances in the blood crystallize in the kidneys and form a solid [3]. If left unchecked, kidney stones can cause problems such as infection, blockage of the flow of urine and can even damage the kidneys. Therefore, it is necessary to make a proper diagnosis in patients with kidney stones.

Ultrasonography (USG) is a diagnostic method in which ultrasonic images are created by very high frequency sound waves, which have an acoustic frequency above the threshold of human hearing [4]. In the medical world, ultrasound is used by medical personnel for imaging in pregnancy and diagnosing internal organs, one of which is renal ultrasound (kidney ultrasound). The way kidney ultrasound works are the same as regular ultrasound, namely by utilizing ultrasonic waves, but the difference from uterine ultrasound is the object being observed or an image taken. On a kidney ultrasound, an image of the kidney is taken. The sensitivity and specificity of ultrasound for renal abnormalities are quite high, namely 66.7% and 97.4% respectively [5]. Due to its sensitivity, renal ultrasound examination has become a substitute for other diagnostic mechanisms as an initial diagnostic action.

To identify kidney stones, the doctor will first try to gather information from the patient about the patient's symptoms. Once the information is gathered, several test options will be run to confirm the diagnosis. These tests include urinalysis, blood tests, and scans (eg ultrasound, intravenous

urography/IVU, x-ray, and CT scan). Most patients with kidney disease go for an ultrasound scan because it is cheaper and does not require special requirements such as fasting before having the scan. After an ultrasound scan is performed, the resulting image will be identified by the naked eye by an expert or a doctor manually.

Several studies related to detection, entitled Implementation of Gabor Wavelet and Support Vector Machine on Polycystic Ovary (PCO) Detection in 2016. The research entitled Implementation of Gabor Wavelet and Support Vector Machine on Polycystic Ovary (PCO) Detection Based on Ultrasonographic Imagery was conducted by Untari Novia Wisesty and Titik Mutiah in 2016. Before identification, image pre-processing and feature extraction were carried out using Gabor Wavelet. In classifying, the method used is Support Vector Machine with an accuracy of 78.466% [6].

Other research, entitled Analysis and Identification of Kidney Stone Using K-Nearest Neighbor (KNN) and Support Vector Machine (SVM) Classification Techniques was conducted by Jyoti Verma, et al in 2017. Before being identified, the steps taken were image pre-processing and segmentation to find ROI. (Regions of Interest). The classification method in this study is K-Nearest Neighbor (KNN) and Support Vector Machine (SVM) and achieves an accuracy of 89% on KNN and 84% on SVM [7].

We also reviewed other research related to extreme learning machine implementation on several area. For example, in 2020, the research entitled Fruits Classification from Image using MPEG-7 Visual Descriptors and Extreme Learning Machine was conducted by Joko Siswantoro, at al. The best classification performance of 97.33% has been achieved in classifying Indonesian fruit images consisted using 3000 fruit images of 15 classes. By applying the ensemble of ELMs, the classification accuracy was increased to 98.03%. This result shows that the proposed method produces high classification performance. Furthermore, the experiment result also shows that ELM outperforms k-NN and LDA [8].

The next research entitled Breast cancer diagnosis using an enhanced Extreme Learning Machine Based-Neural Network was conducted by Mohamed Nemissi, at al [9]. The aim of this work it to introduce a system for classifying breast cancer based on an enhanced single hidden neural network trained using ELM algorithm. The proposed enhancement is based on the activation functions. They used sigmoid activation functions with different parameters for the hidden neurons. In this research with Extreme Machine Learning method can classify Breast cancer very well with an accuracy of 97.28%.

Since our study also related to ultrasound images, we also review a study related to identification of the disease through the ultrasound images. The research entitled Diagnosis of Renal Calculus Disease in Medical Ultrasound Images was conducted by Prema T. Akkakaligar and Sunanda Biradar in 2016. In this study, the stages of image processing were Speckle Noise Removal, Wavelet Processing then feature extraction and segmentation using Seed Region Growing. After that, the image classification uses a Multilayer Feed-forward Artificial Neural Network. This study obtained an accuracy of 96.88% [10].

Based on the previous research background that has been described, we find a research gap, that in identifying kidney stone images, there is still a gap to get higher accuracy compared to KNN or SVM [7] by using ELM. ELM is a very good method to do image classification, and also, this study will answer is ELM suitable in identifying kidney stone images. Therefore, we had initiative to conduct research that can produce applications that can facilitate the process of detecting kidney stones in kidney ultrasound images using the Extreme Learning Machine. Extreme Learning Machine is a learning method that is still relatively new in an artificial neural network which also can conduct prediction experiment not just a classification tools [11]. This method was first introduced in 2004 by Huang G.B [12]. Extreme Learning Machine is one of the solutions because it has advantages in terms of speed of training time and also higher accuracy that can be achieved compared to traditional machine learning methods.

2. METHODOLOGY

In the process of carrying out this research, the data used were ultrasound photos of normal kidneys and kidney stones. The data was collected by researchers from Harapan Pematangsiantar Hospital and Vita Insani Hospital in Pematangsiantar and has been validated by Dr. Harlen Saragih, SP. Rad and Dr. Efrilyn Sidabutar, SpPD. Then the data is divided into two categories, namely normal kidney ultrasound images and kidney stones. In this study, 139 datasets were used, with a total of 113 training

data and 26 testing data, where the ratio of training data: testing data was 70: 30. Image division is shown in Table 1.

Table 1. Distribution of Training and Testing Data

No.	Disease Name	Amount of data	
		Train Data	Test Data
1	Normal	15	43
2	Kidney Stones	11	70
	Total	26	113

The stages of the research carried out in this study consisted of image acquisition, image pre-processing, image segmentation, feature extraction, and identification using an Extreme Learning Machine. The general architecture that describes the stages carried out can be seen in Figure 1.

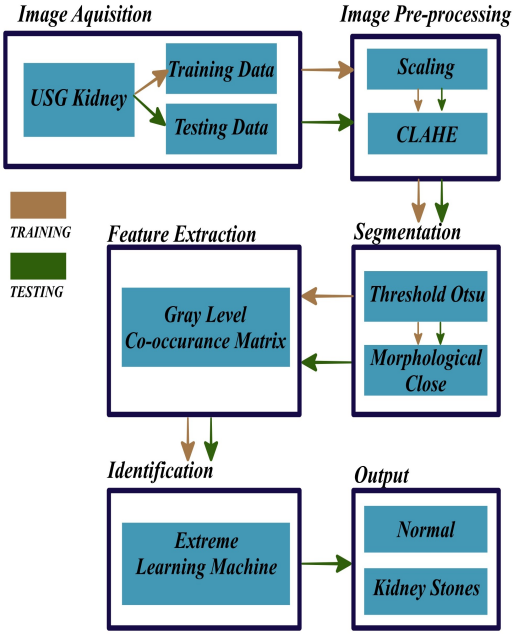

Figure 1 : General Architecture

From the image above, the first stage is Image Acquisition. At this stage the data is acquired to be used as a training image as well as a test image. After that, the image pre-processing stage is carried out which is divided into scaling which is used to reduce the size of the image and CLAHE to increase the quality of contrast in the image. The next stage is segmentation using the Otsu threshold and morphological close. Then proceed with the feature extraction process Gray Level Co-occurrence Matrix then the identification stage using Extreme Machine Learning.

.

3.1 Image Acquisition

This study used kidney ultrasonography (USG) images obtained from several hospitals in North Sumatra, Indonesia. In this study, the image used .JPG extension and data were divided into two categories, namely normal kidney ultrasound images and kidney stones. In this research, we used a dataset of 139 images, with training data of 113 images and testing data with a total of 26 images. An example of a kidney USG image can be seen in Figure 2.

Figure 2 : USG Image of a kidney

3.2 Image Pre-processing

The first stage in Image Pre-processing is scaling. The purpose of scaling is to adjust the image pixels to be similar in size. Image processing time will be less if the number of pixels is getting smaller. In this study, the image is resized to 300 x 300 pixels. Next in the image pre-processing step is contrast limited adaptive histogram equalization (CLAHE). This stage aims to adjust the intensity of the image contrast so that the invisible or dark parts can be displayed.

The following are the stages of how CLAHE works on images [13]:

Step 1: At this stage, the image is divided into components called tiles of MxN size

Step 2 : At this stage the histogram on each tile will be calculated

Step 3: Then at this stage a clipped histogram will be carried out. The number of pixels of each tile is distributed equally at each gray level.

Step 4 : Then at this stage the contrast histogram will be limited in each tile, then by using bilinear interpolation, each tile is connected. To calculate the clip limit on a histogram, Equation (1) can be used.

$$\beta = \frac{M}{N}\left(1 + \frac{a}{100}(s-1)\right) \quad (1)$$

Where :
M = Area Region Size
N = Gray level value
α = clip factor value

The image of the results of the CLAHE process can be seen in Figure 3.

Figure 3 : USG Image of a kidney after CLAHE

3.3 Segmentation

In the segmentation stage, consisting of determining the Otsu threshold, the Otsu threshold method is a method that can find threshold values in digital images automatically by performing a discriminant analysis of the histogram gray level which is expected to be able to separate objects (foreground) and background (background) independentl, precise and optimal [14]. The first step in segmentation is the otsu threshold. This step is carried out to separate the object (foreground) and the background (background). It is based primarily on the image histogram, looking at the values of pixel and the regions to segment out, rather than the image edges. It tries segmenting it by making the variance on each of the minimal classes [15].

For example, k states the threshold value to be searched for. The value of k varies from 1 to L, where L = 255. Equation (2) states the probability for pixel l.

$$P_i = \frac{n_i}{N} \quad (2)$$

The number of pixels is expressed by n_i with gray level I and the number of image pixels is expressed by N. The value of the cumulative moment to zero, cumulative moment to one, and the mean (average) value can be expressed sequentially using Equations (3), (4), and (5).

$$\omega(k) = \sum_{i=1}^{k} Pi \quad (3)$$

$$\mu(k) = \sum_{i=1}^{k} i.Pi \quad (4)$$

$$\mu_T(k) = \sum_{i=1}^{L} i.Pi \quad (5)$$

The following is the equation for calculating the k threshold value:

$$\delta_B^2(k^*) = max_{1 \le k < L} \delta_B^2(k) \quad (6)$$

With :

$$\delta_B^2(k) = \frac{[\mu T \omega(k) - \mu(k)]^2}{\omega(k)[1 - \omega(k)]} \quad (7)$$

Where :

P_i	:	Pixel probability
n_i	:	the number of pixels in the gray level
N	:	number of image pixels
k	:	number of image pixel
ω	:	cumulative moment
μ	:	average value
μ_T	:	average value
δ	:	class variance

The resulting image of the Otsu threshold process can be seen in Figure 4.

Figure 4 : USG image of a kidney after threshold otsu

After going through the OTSU threshold stage, the image will be processed using the Close

Morphological technique to improve the segmented image. The morphological close image results are divided into 2 categories, namely Dilation and Erosion.

3.3.1. Dilation

Dilation is used to add pixels at region boundaries or to fill in holes in the image. Dilation can also be used to connect disjoint pixels and add pixels at edges [16]. Dilation calculations can be seen using Equation (8).

$$D(A.B) = A \oplus B = \{x : B_x \cap A \neq \emptyset\} \quad (8)$$

Where:

D : image of the result of dilation
A : input image
B : structure elements
Bx : translation B

USG image of the kidney after going through the Dilation process can be seen in Figure 5.

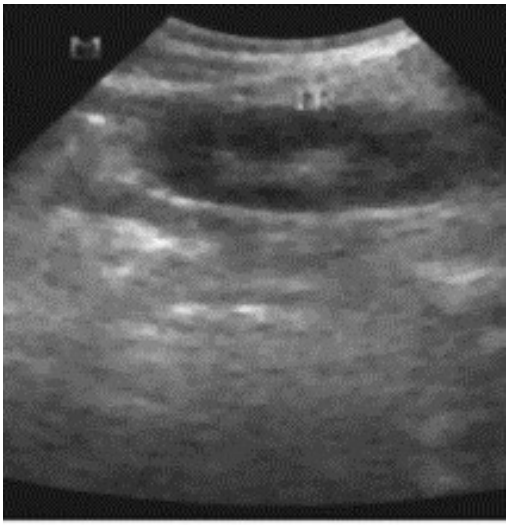

Figure 5. USG image of a kidney after dilation

3.3.2. Erosion

Erosion performs the reverse operation of dilation. When widening widens the boundaries and fills voids, reducing erosion boundary and increase the size of the hole [16]. Erosion calculations can be seen using Equation (9).

$$E\ (A.B) = \mathrm{A}\ \theta\ \mathrm{B} = \{x : B_x \cap X\} \quad (9)$$

Where :

E : erosion result image
A : input image
B : structure elements
Bx : translation

USG image of a kidney after going through the Dilation process can be seen in Figure 6.

3.4 Feature Extraction

At this stage, one of its features will be extracted from the image, namely texture feature extraction using Gray Level Co-occurrence Matrix (GLCM). The GLCM method is a method that has been developed for a long time for texture extraction which is applied to various images. This GLCM method describes the spatial dependence of the gray level on the presented two-dimensional image and captures second-order statistics on gray level gradients (Lam, Cheung & Stephen Wang, 1996).

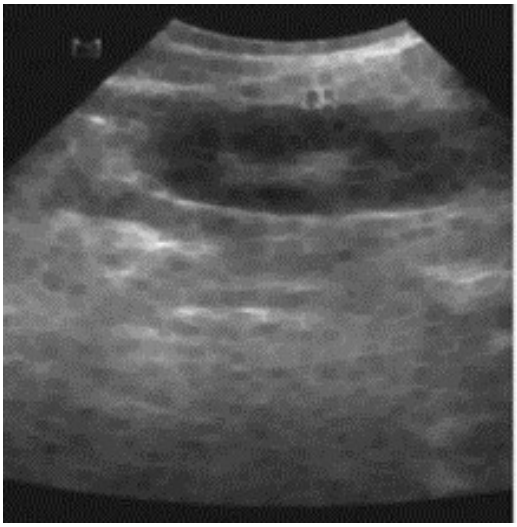

Figure 6. USG Image of a kidney after Erosi

The image to be extracted is a type of gray degree image and converted into a GLCM matrix where this matrix is a matrix representing the relationship between neighboring pixels (in various directions) with spatial distance. The steps in this extraction are:

1. Set the gray-level image to be the size of the GLCM matrix
2. Set the spatial distance and orientation angle between pixels. In this study the spatial distance (d) used is 1 and uses 4 angles, namely 0˚, 45˚, 90˚and 35˚.
3. The co-occurrence value will be calculated based on predetermined distances and angles.
4. To produce a symmetric co-occurrence matrix, add the co-occurrence matrix and the transpose matrix
5. Normalize the co-occurrence matrix into probability form by dividing each co-occurrence value by the sum of all the co-occurrence values in the matrix so that the sum of all matrix values has a value of 1.

6. Calculating texture feature values using entropy, contrast, correlation, energy and homogeneity methods.
   a. Entropy
      To calculate entropy, you can use Equation (10).

$$Entropy = \sum_{i,j} p(i,j) \log(p(i,j)) \quad (10)$$

   b. Contrast
      To calculate the contrast, you can use Equation (11).

$$Contrast = \sum_{i,j} |i-j|^2 \, p(i,j) \quad (11)$$

   c. Correlation
      To calculate correlation, you can use Equation (12).

$$Correlation = \frac{\sum_i - \sum_j (ij)\, p(i,j) - \mu_x \mu_y}{\sigma_x \sigma_y} \quad (12)$$

   d. Energy
      To calculate energy, you can use equation (13).

$$Energy = \sum_{i,j} p(i,j) \quad (13)$$

   e. Homogeneity
      To calculate homogeneity, you can use Equation (14).

$$Homogeneity = \sum_{i,j} \frac{p(i,j)}{1+|i-j|} \quad (14)$$

The calculation results of each method above will be replaced into a column vector. There are 4 matrices in GLCM based on the angles that have been done before and each of these matrices forms 5 texture features so that there are a total of 20 features which will then be used as input so that it can be processed by ELM.

3.5 Identification

Extreme learning machine is an artificial neural network with feedforward character which has a single hidden layer where there is only one hidden layer [17]. Huang et al (2006) stated that the extreme learning machine learning method was created to overcome the deficiencies in feedforward neural networks, most importantly in terms of learning speed, which is currently happening in Feedforward Neural Networks [18].

There are two reasons for the deficiencies in Feedforward neural networks, most importantly in terms of learning speed:

1. Feedforward neural networks in carrying out the training process use a slow gradient based learning algorithm.
2. Determination of all parameters in the network is done iteratively or repeatedly using the learning method.

Determination of all parameters in a feedforward artificial neural network must be done manually when using conventional gradient based learning algorithms such as backpropagation. The parameters here are hidden bias and input weight where one layer is related to another, which ultimately requires a long learning speed and is often trapped in local minima. Meanwhile, the parameters in the extreme learning machine such as hidden bias and input weight are set randomly. Therefore, the learning speed possessed by extreme learning machines is shorter or faster and can obtain more optimal performance.

The mathematical model of a feedforward artificial neural network is different from the Extreme learning machine. In Extreme learning machine, the mathematical model is more effective and simple. In Equation (15) it can be seen that for N different numbers of samples, the extreme learning machine (Xi, ti) mathematical model is as follows:

$$X_i = [X_{i1}, X_{i2}, \ldots, X_{in}]^T \in R^n$$

$$X_t = [X_{t1}, X_{t2}, \ldots, X_{tn}]^T \in R^m \quad (15)$$

The following is a systematic overview of the SLFNs standard where the number of hidden nodes is N and the activation functions are g(x) :

$$\sum_{i=1}^{N} \beta_i g_i(x_j) - \sum_{i=1}^{N} \beta_i g(w_1 x_j + b_i) - o_j \quad (16)$$

Where :

j = 1,2,…,N

$w_i = (w_{i1}, w_{i2}, \ldots, w_{in})^T$ is a vector of weight that connects hidden nodes i and input nodes.

$i = (i1, i2, \ldots, im)^T$ is the weight vector that connects hidden nodes i with output nodes.

b_i = threshold of hidden nodes i.

$w_i \cdot x_j$ = *inner product* from w_i and x_j

Wang et al (2011) stated that SLFNs with N hidden nodes and activation function g(x) are expected to be able to predict with an error level of 0 [19], or can be written in Equation (17).

$$\sum_{j=1}^{N} \|o_j - t_j\| = 0 \text{ then } o_j = t_j$$
$$\sum_{i=1}^{N} \beta i g(w_i \cdot x_j + b_i) = t_j \quad (17)$$

The above equation can be simplified into :

$$H\beta = T \quad (18)$$

Where :
H = *hidden layer output* matrix
β = *output weight*
T = matrix of targets or outputs

In extreme learning machine, hidden bias and input weight are assigned randomly. Then the output weight that is connected to the hidden layer can be found by the equation :

$$\beta = H^{+}T \quad (19)$$

H^{+} is the Moore-Penrose Generalized Inverse matrix of the H matrix. The H matrix is a matrix that is arranged based on the output of each hidden layer. Meanwhile T is the target matrix.

Identification process using Extreme Learning Machine. The Extreme Learning Machine architecture consists of 3 layers, namely an Input Layer of 20 nodes, a Hidden Layer of 20 nodes, and an Output Layer of 2 nodes (Normal and Kidney Stones). The architecture of the Extreme Learning Machine in this study can be seen in Figure 7.

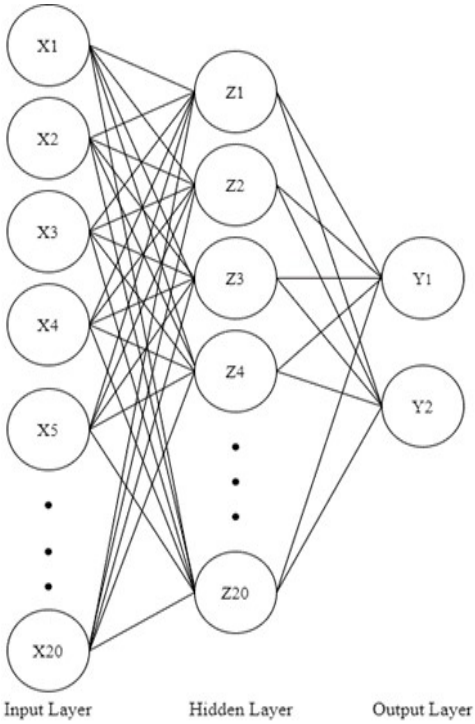

Figure 7 : Extreme Learning Machine Architecture

The number of values from the feature extraction results will determine the number of nodes in the input layer. However, the best accuracy in the kidney stone identification system is obtained by selecting the number of weights as many as 40 nodes.

The following are the training stages that will be processed:

Step 1: Initialize all weights and bias using small random numbers [0-1].

Step 2: If the termination status has not materialized, proceed to Stage 3 to Stage 7

Phase I of forward propagation (feed forward):

Step 3: The signal will be received by each input unit Xi (i = 1, 2, …, n) and the signal is forwarded to all hidden layers.

Step 4: Calculate each hidden unit layer Zj (j = 1, 2, …, m) by summing the weighted input signals.

$$z\_net_{j=} b_j + \sum_i^n \mathbf{1}\, x_i w_{ji} \quad (20)$$

Next, using the binary sigmoid activation function, calculate the output in the hidden layer.

$$g\left(z_{net_j}\right) = \frac{1}{1 - e^{-z_{net\,j}}} \quad (21)$$

If the output on the hidden layer has been obtained, then proceed to the next stage.

Step 5: Calculate the H matrix of size n x m.

$$H \begin{pmatrix} g(x_1w_{11}+b_{10}) & g(x_1w_{12}+b_{20}) & g(x_1w_{13}+b_{30}) & g(x_1w_{14}+b_{40}) \\ g(x_2w_{21}+b_{10}) & g(x_2w_{22}+b_{20}) & g(x_2w_{23}+b_{30}) & g(x_2w_{24}+b_{40}) \\ g(x_3w_{31}+b_{10}) & g(x_3w_{32}+b_{20}) & g(x_3w_{33}+b_{30}) & g(x_3w_{34}+b_{40}) \\ g(x_4w_{41}+b_{10}) & g(x_4w_{42}+b_{20}) & g(x_4w_{43}+b_{30}) & g(x_4w_{44}+b_{40}) \\ g(x_5w_{51}+b_{10}) & g(x_5w_{52}+b_{20}) & g(x_5w_{53}+b_{30}) & g(x_5w_{54}+b_{40}) \end{pmatrix} \quad (22)$$

If the H matrix of size n x m has been obtained, calculate H+ which is the pseudoinverse matrix of the H matrix which will be used in tracing the weights of the hidden layer or output layer. The following is the equation *H+* :

$$H^{+} = (H^{T}H)^{-1}H^{T} \quad (23)$$

Then find the weight to the output layer (β)

$$\beta = H^{+}t_1 \quad (24)$$

Step 6 : Calculate the output value using equation 17.

$$\sum_{j=1}^{m} \beta_j g(z_{net})_j = y \quad (25)$$

Step 7 : Calculate the error value at the output unit using equation 18.

$$E = \|y - t_j\| \quad (26)$$

Phase II Changes update weights and biases

Step 8 : Calculate the overall weight shift and the bias associated with the hidden layer unit.

$$w_{ij(new)} = w_{ij(old)} + \alpha\delta_j x_i \quad (27)$$

ISSN: 1992-8645 www.jatit.org E-ISSN: 1817-3195

Step 9: Check the state of the stop. In the training process, the iteration stops if the epoch is smaller than the epoch max that has been set.

Step 10: Storage of appropriate or optimal bias weights

Example of Extreme Learning Machine process (20 hidden layer nodes) :

1. Initialize all biases and weights using small random numbers [0-1].
2. If the state of termination has not materialized, then stage 3 - stage 7 is carried out.
3. Calculate the output in the hidden layer.
   - Calculate the value of z_netj where j = 20 nodes in the hidden layer using Equation (20):

$$z_{net_1} = b_1 + x_1w_{11} + x_2w_{21} + \cdots + x_{20}w_{201}$$

$$= 0.1 + (0{,}18\,.\,0{,}4) + (0{,}9\,.\,0{,}1) + (0{,}1\,.\,0{,}3) + \ldots + (0{,}8\,.\,0{,}2)$$

$$= 0.875$$

   - Then calculate the output value zj at the nodes in the hidden layer using the binary sigmoid activation function

$$z_1 - f(z_{net_1}) - \frac{1}{1 + e^{-(0.875)}} - 0{,}705$$

$$z_2 = f(z_{net_2}) = \frac{1}{1 + e^{-(0.956)}} = 0{,}722$$

4. The activation function will get the result which is the input for the hidden layer. Then the process after that is the calculation of the output weight. In calculating the output weight, equation (16) is used.

$$H = \begin{pmatrix} g(x_1w_{11} + b_1) & g(x_1w_{12} + b_2) \\ g(x_2w_{21} + b_1) & g(x_2w_{22} + b_2) \\ g(x_3w_{31} + b_1) & g(x_3w_{32} + b_2) \\ \vdots & \vdots \\ g(x_{20}w_{201} + b_1) & g(x_{20}w_{202} + b_2) \end{pmatrix}$$

$$g(x_1w_{11} + b_1) = (0{,}18\,.\,0{,}4) + 0{,}1 = 0.542$$

$$g(x_2w_{21} + b_1) = (0{,}9\,.\,0{,}1) + 0{,}1 = 0.547$$

$$g(x_3w_{31} + b_1) = (0{,}1\,.\,0{,}3) + 0{,}1 = 0.532$$

$$g(x_{20}w_{201} + b_1) = (0{,}8\,.\,0{,}2) + 0{,}1 = 0.564$$

$$g(x_1w_{12} + b_2) = (0{,}18\,.\,0{,}2) + 0{,}2 = 0.558$$

$$g(x_2w_{22} + b_2) = (0{,}9\,.\,0{,}4) + 0{,}2 = 0.636$$

$$g(x_3w_{32} + b_2) = (0{,}1\,.\,0{,}6) + 0{,}2 = 0.564$$

$$g(x_3w_{32} + b_2) = (0{,}1\,.\,0{,}6) + 0{,}2 = 0.564$$

$$H = \begin{pmatrix} 0{,}542 & 0{,}558 \\ 0{,}547 & 0{,}636 \\ 0{,}532 & 0{,}564 \\ \vdots & \vdots \\ 0{,}564 & 0{,}645 \end{pmatrix}$$

5. Next find the value of β using Equations (23) and (24).

$$= \left(\begin{pmatrix} 0{,}542 & 0{,}547 & 0{,}532 & \ldots & 0{,}564 \\ 0{,}558 & 0{,}636 & 0{,}564 & \ldots & 0{,}645 \end{pmatrix} \begin{pmatrix} 0{,}542 & 0{,}558 \\ 0{,}547 & 0{,}636 \\ 0{,}532 & 0{,}564 \\ \vdots & \vdots \\ 0{,}564 & 0{,}645 \end{pmatrix} \right)^{-1}$$

$$= (1.449, 1.312, \ldots, 1.193)$$

6. The stage of calculating the output value using the Equation (25).

$$y_1 = f(y_{net_1}) = \frac{1}{1 + e^{-(0.658)}} = 0{,}658$$

7. The stage of calculating the error using the Equation (26).

$$E = \|y - t\| = \|0{,}658 - 1\| = 0{,}342$$

8. The stage of updating the weight value using the Equation (27).
   - Sum of errors in the hidden layer δ_net_j

$$\delta\_net_1 = E\,\beta_1 = 0{,}342\,.\,1{,}449 = 0{,}495$$

$$\delta\_net_2 = E\,\beta_2 = 0.342\,.\,1{,}312 = 0{,}448$$

   - Calculate the error factor in the hidden layer δ_j.

$$\delta_1 - \delta_{net_1} z_1(1 - z_1) - (0{,}495)(0{,}705)(1 - 0{,}705) - 0{,}754$$

$$\delta_1 = \delta_{net_2} z_2(1 - z_2) = (0{,}448)(0{,}722)(1 - 0{,}722) = 0{,}766$$

   - Calculate the new weight of each hidden layer node using Equation (27).

$$W_{ij(new)} = W_{ij(old)} + \alpha\delta_j x_i$$

$$W_{11(new)} = 0{,}4 + (0{,}1)(0{,}754)(0{,}18) = 0{,}413$$

$$W_{12(new)} = 0{,}2 + (0{,}1)(0{,}766)(0{,}9) = 0{,}268$$

From the results of the calculation of the new weight, then continue the calculation starting from Stage 3 to 7 until the stopping state is reached. If the epoch is less than the specified epoch max, then the iteration in the training process will stop. Then save the appropriate or optimal bias weights. Then enter the testing stage to test the accuracy of the system. These are the stages :

1. Input the data being tested.
2. Input the ideal hidden node value from the training data.

ISSN: 1992-8645 www.jatit.org E-ISSN: 1817-3195

3. Carry out the feedforward process, namely calculating the output output. Because sigmoid binary is used in this network, the output range is [0,1].
4. The output results are analyzed
5. Drawing conclusions based on the output results.

3. TESTING AND RESULT

The stages of the research carried out in this study consist of image acquisition, image pre-processing, image segmentation, feature extraction, and identification using. The data training process will affect the ability of the system being built. Tests on various hidden neurons were carried out on the system, namely n=10, n=15, n=20, n=40. The sigmoid function is used for data testing results using 10, 15, 20, and 40 neurons, with learning rate 0.2 and epoch 1000.

Test results with the Sigmoid activation function on 26 test data can be seen in Table 2 below.

Table 2 : Test Results with Sigmoid

No	File Name	Sigmoid Activation Function			
		10 Neuron	15 Neuron	20 Neuron	40 Neuron
1	bg_1	Kidney Stones	Kidney Stones	Kidney Stones	Kidney Stones
2	bg_2	Kidney Stones	Kidney Stones	Kidney Stones	Kidney Stones
3	bg_3	Normal	Kidney Stones	Kidney Stones	Kidney Stones
4	bg_4	Kidney Stones	Normal	Kidney Stones	Kidney Stones
5	bg_5	Kidney Stones	Normal	Kidney Stones	Kidney Stones
6	bg_6	Kidney Stones	Kidney Stones	Kidney Stones	Kidney Stones
7	bg_7	Kidney Stones	Normal	Kidney Stones	Kidney Stones
8	bg_8	Kidney Stones	Normal	Normal	Kidney Stones
9	bg_9	Kidney Stones	Normal	Normal	Kidney Stones
10	bg_10	Kidney Stones	Normal	Normal	Kidney Stones
11	bg_11	Normal	Kidney Stones	Normal	Normal
12	n_1	Normal	Normal	Normal	Normal
13	n_2	Kidney Stones	Normal	Normal	Normal
14	n_3	Normal	Normal	Normal	Normal
15	n_4	Kidney Stones	Normal	Normal	Normal
16	n_5	Kidney Stones	Normal	Normal	Normal
17	n_6	Kidney Stones	Normal	Normal	Normal
18	n_7	Kidney Stones	Normal	Normal	Normal
19	n_8	Normal	Normal	Normal	Normal
20	n_9	Kidney Stones	Normal	Normal	Normal
21	n_10	Kidney Stones	Kidney Stones	Normal	Normal
22	n_11	Kidney Stones	Kidney Stones	Normal	Kidney Stones
23	n_12	Kidney Stones	Normal	Normal	Normal
24	n_13	Kidney Stones	Normal	Normal	Normal
25	n_14	Kidney Stones	Normal	Normal	Normal
26	n_15	Kidney Stones	Kidney Stones	Kidney Stones	Normal
Accurate image		11	16	21	24
Inaccurate image		10	10	5	2

From the results of testing the data, the test results can be seen in table 3 below.

Tabel 3: Testing Result

Number of training data	Number of testing data		Number of hidden neurons	Accuracy
	True	False		
113	11	10	10	42.31%
113	16	10	15	61.54%
113	21	5	20	80.77%
113	24	2	40	92.30%

Based on the test accuracy table, it shows that better accuracy will be obtained at a higher number of hidden neurons. The accuracy obtained in hidden neuron 10 is 42.31% with 10 false images and 11 correct images. Then the accuracy obtained in hidden neuron 15 is 61.54% with 10 false images and 16 correct images. While the accuracy reaches

80.77% on hidden neuron 20 which then makes accuracy on hidden neuron 20 with 5 false images and 21 correct images. Then, we try to increase the hidden neuron into 40, and we received the accuracy increment that reaches 92.30% with 2 wrong images and 24 correct images classified correctly.

Based on this finding we can see that the increment of hidden neurons number will increase the accuracy of the dataset, and effecting the training time. However, since ELM is designed to reduced training time, then it should not be a matter in this case. The limitation of the data also one of the factors that the accuracy can be greater than this result. It is because more data will give more accuracy.

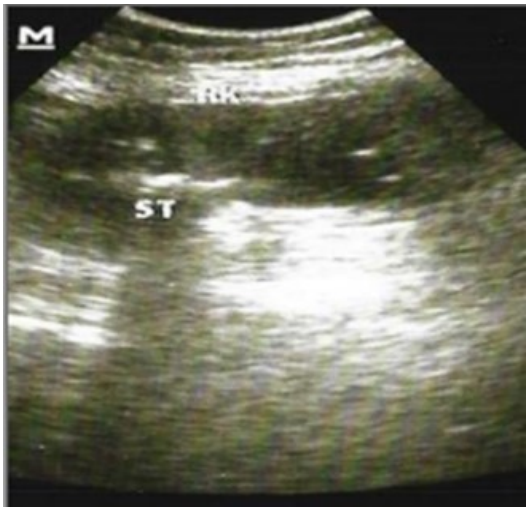

Figure 8. Misidentified Kidney Stone Image

Figure 9. Normal Image similar to Kidney Stones.

In the kidney stone identification system there are still imperfections, namely the system sometimes still makes mistakes in identifying. The factor for this error is the lack of training data and the similarity of the image data used for this study. An example of an image that the system failed to identify can be seen in Figure 8.

Figure 9 is an image of a kidney stone but the system made an error in the identification process which then caused the identification results to be normal. The reason for this is that the image processing stage is still inaccurate in taking disease characteristics. Another reason is that the shape of kidney stones and normal kidneys are similar, which makes it difficult for the system to identify them. In Figures 8 and 9 it can be seen that the images of kidney stones and normal kidneys are similar.

4. CONCLUSION

Based on the research results, a computational system for identifying kidney stones using the Extreme Machine Learning (ELM) method can identify kidney images with an accuracy of 92.30%. This accuracy has outperformed SVM and KNN classification used in previous research. Based on the results of system testing as well, the number of hidden neurons greatly influences the accuracy of identification in the system. The best system accuracy is obtained by using 40 hidden nodes in identifying kidney stones using the Extreme Machine Learning method. In addition, the time needed for data training will increase if the number of hidden nodes is increased. Using more training data makes it possible to have a variety of features in the image data thereby increasing accuracy when testing. Using other image pre-processing processes is also possible to improve image quality, especially in the dark and light parts of the image. We also can conclude that ELM is superior compared to SVM or ANN in identifying kidney stones images. This will contribute to health specialist in minimizing their decision after read kidney stone USG images.

ACKNOWLEDGMENT:

The authors would like to thank profusely for the financial support provided by DIPA funds Polmed (Politeknik Negeri Medan) to carry out research with contract number: B/443/PL5/PT.01.05/2023. The funds received from the DIPA POLMED gives a very important role in the successful completion of this study.

ISSN: 1992-8645 www.jatit.org E-ISSN: 1817-3195

REFERENCES:

[1] C. f. D. Control and Prevention, "Chronic kidney disease in the United States, 2019," *Atlanta, GA: US Department of Health and Human Services, Centers for Disease Control and Prevention,* vol. 3, 2019.

[2] S. Nurjanah, F. N. Damayanti, and A. A. Riafisari, "Differences of Menstrual Cycle Before and After Hemodialysis in Women Suffering Chronic Kidneys," *Turkish Journal of Computer and Mathematics Education (TURCOMAT),* vol. 12, no. 13, pp. 6459-6465, 2021.

[3] U. Atodariya, R. Barad, S. Upadhyay, and U. Upadhyay, "Anti-urolithiatic activity of Dolichos biflorus seeds," *Journal of Pharmacognosy and Phytochemistry,* vol. 2, no. 2, pp. 209-213, 2013.

[4] F. Caglayan and I. S. Bayrakdar, "The intraoral ultrasonography in dentistry," *Nigerian journal of clinical practice,* vol. 21, no. 2, pp. 125-133, 2018.

[5] N. P. Roberson *et al.*, "Comparison of ultrasound versus computed tomography for the detection of kidney stones in the pediatric population: a clinical effectiveness study," *Pediatric radiology,* vol. 48, pp. 962-972, 2018.

[6] U. N. Wisesty, "Implementasi Gabor Wavelet dan Support Vector Machine pada Deteksi Polycystic Ovary (PCO) Berdasarkan Citra Ultrasonografi," *Indonesia Journal on Computing (Indo-JC),* vol. 1, no. 2, pp. 67-82, 2016.

[7] J. Verma, M. Nath, P. Tripathi, and K. Saini, "Analysis and identification of kidney stone using K th nearest neighbour (KNN) and support vector machine (SVM) classification techniques," *Pattern Recognition and Image Analysis,* vol. 27, pp. 574-580, 2017.

[8] J. Siswantoro, H. Arwoko, and M. Z. F. N. Siswantoro, "Fruits Classification from Image using MPEG-7 Visual Descriptors and Extreme Learning Machine," in *2020 3rd International Seminar on Research of Information Technology and Intelligent Systems (ISRITI)*, 2020, pp. 682-687.

[9] N. M, S. H, and S. H, "Breast cancer diagnosis using an enhanced Extreme Learning Machine based-Neural Network," in *2018 International Conference on Signal, Image, Vision and their Applications (SIVA)*, 2018, pp. 1-4.

[10] P. T. Akkasaligar and S. Biradar, "Diagnosis of renal calculus disease in medical ultrasound images," in *2016 IEEE International Conference on Computational Intelligence and Computing Research (ICCIC)*, 2016, pp. 1-5: IEEE.

[11] F. Rahmat Romi, B. Pangaribuan Artambo, E. Suwarno, S. Purnamawati, and Z. Lini Tifani, "Lake Toba Water Quality Prediction Using Extreme Machine Learning," *ICIC Express Letters, Part B: Applications,* vol. 13, no. 01, p. 89, 2022 2022.

[12] M. I. Sa'ad, Kusrini, and M. S. Mustafa, "Student Prediction of Drop Out Using Extreme Learning Machine (ELM) Algorithm," in *2020 2nd International Conference on Cybernetics and Intelligent System (ICORIS)*, 2020, pp. 1-6.

[13] N. NURZAENAB, M. S. HADIS, and R. ANGRIAWAN, "Nilai Optimal Clip Limit Metode Clahe Untuk Meningkatkan Akurasi Pengenalan Wajah Pada Video Cctv," *Jurnal INSTEK (Informatika Sains dan Teknologi),* vol. 5, no. 2, pp. 178-187, 2020.

[14] Q. Huang, W. Gao, and W. Cai, "Thresholding technique with adaptive window selection for uneven lighting image," *Pattern Recognition Letters,* vol. 26, no. 6, pp. 801-808, 2005/05/01/ 2005.

[15] H. E. Khoukhi, Y. Filali, A. Yahyaouy, M. A. Sabri, and A. Aarab, "A hardware Implementation of OTSU Thresholding Method for Skin Cancer Image Segmentation," in *2019 International Conference on Wireless Technologies, Embedded and Intelligent Systems (WITS)*, 2019, pp. 1-5.

[16] N. Jamil, T. M. T. Sembok, and Z. A. Bakar, "Noise removal and enhancement of binary images using morphological operations," in *2008 International Symposium on Information Technology*, 2008, vol. 4, pp. 1-6.

[17] J. Wang, S. Lu, S.-H. Wang, and Y.-D. Zhang, "A review on extreme learning machine," *Multimedia Tools and Applications,* vol. 81, no. 29, pp. 41611-41660, 2022/12/01 2022.

[18] G.-B. Huang, Q.-Y. Zhu, and C.-K. Siew, "Extreme learning machine: Theory and applications," *Neurocomputing,* vol. 70, no. 1, pp. 489-501, 2006/12/01/ 2006.

[19] Y. Wang, F. Cao, and Y. Yuan, "A study on effectiveness of extreme learning machine," *Neurocomputing,* vol. 74, no. 16, pp. 2483-2490, 2011/09/01/ 2011.